Field Enhancement of a Superconducting Helical Undulator with Iron

K. Flöttmann, S.G. Wipf
DESY, Notkestr. 85, 22603 Hamburg, Germany

Introduction

The productions of positrons in sufficient quantities is one of the necessities for either the TESLA or the S-Band Linear Collider project. One of the promising possibilities is to guide the high energy electron beam through a superconducting helical undulator producing synchrotron radiation which would in turn be directed onto a target for positron production [1].
A helical undulator has two advantages as compared to a planar wiggler: The energy of the primary electron beam can be lower, since high photon energies can be reached with a short period, high field device. While a source with a planar wiggler can operate only with a minimum beam energy of at least 150GeV, the operation of a source with a helical undulator seems to be possible down to an energy of ~100-120GeV.
In addition the photons of a helical undulator close to the radiation axis are circularly polarized. Highly polarized positrons can be generated if the outer part of the photon beam is scraped off. Since this requires an overproduction of photons it can in general only be realized at higher energies of the primary electron beam. Thus the same helical undulator could be used for the production of positrons with a low polarization (~30 %) at lower beam energy (~120GeV) and for highly polarized positrons (~60%) at high beam energies ($\geq$250GeV).
Primary calculations (based on an analytical formula for the field of an iron free helical undulator) yield the following undulator parameters[2]:

minimum electron beam energy	~150 GeV
period	λ = 1.2 cm
magnetic field	B = 0.9 T
total undulator length	L = 150 m

In this paper an optimized geometry for an undulator with iron will be presented. We concentrate on the field enhancement due to iron. Questions concerning the technical design of a helical undulator with iron will not be addressed.

Geometry of a helical undulator with iron

A helical field can be produced by a pair of conductors wound to form a double helix as sketched in Figure 1. The current in the two conductors is equal and of opposite direction. Thus the central axial magnetic field is canceled and a transverse field pattern appears. The on-axis field is approximated by:

$$B_x = B \cdot \sin\left(\frac{2\pi z}{\lambda}\right)$$

$$B_y = B \cdot \cos\left(\frac{2\pi z}{\lambda}\right)$$

λ = undulator period

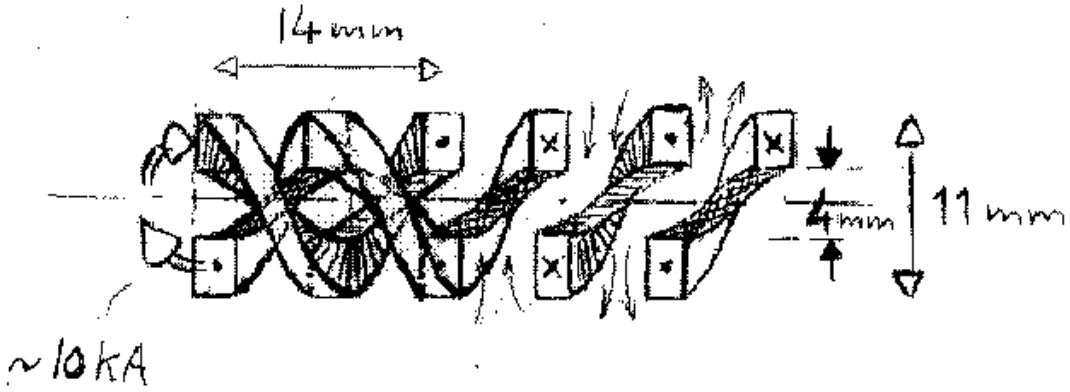

Figure 1 Diagram of an iron free helical undulator. (Picture courtesy of S.L. Wipf.)

An analytical formula for an iron free undulator was derived by Blewett and Chasman [3] as:

$$B = 2.385 \cdot 10^{-4} [T \cdot mm / A] \cdot I \cdot \lambda \cdot \left[e^{\frac{-5.68 \cdot r_i}{\lambda}} - e^{\frac{-5.68 \cdot r_o}{\lambda}} \right] \qquad (1)$$

I = current density
λ = undulator period
r_i = inner radius of the coil
r_o= outer radius of the coil
B = on axis field amplitude

A width of 1/3 λ is assumed for the conductor of the coil. For r_i = 2mm, r_o= 6.8mm, λ=12mm and I = 900A/mm^2 a field of B = 0.9T is reached. In order to include effects of iron the numerical code MAFIA [4] was used. The magnetic field was calculated using the magnetostatic module S. The problem was discretised in a cylindrical coordinate system with 230 000 mesh points. As a first step the analytical result was checked without the addition of iron. The agreement was better than 98 %.

Next a double helix of iron was included between the conductors. Figure 2 shows the undulator with the filaments simulating the conductors and the double helix of iron. The on-axis field was increased by about 50%. Next the undulator was enclosed in a return yoke, which gave another 50% in field amplitude. A variation of the current density between 600 and 900 A/mm^2 revealed no significant limitation due to saturation of the iron. Since the yield of the positron source depends on both the undulator period and the undulator field, the period length of the undulator was reduced to 10mm before the optimization of the geometry. A bore radius r_i of 2mm was chosen, the current density was fixed at 900A/mm^2.

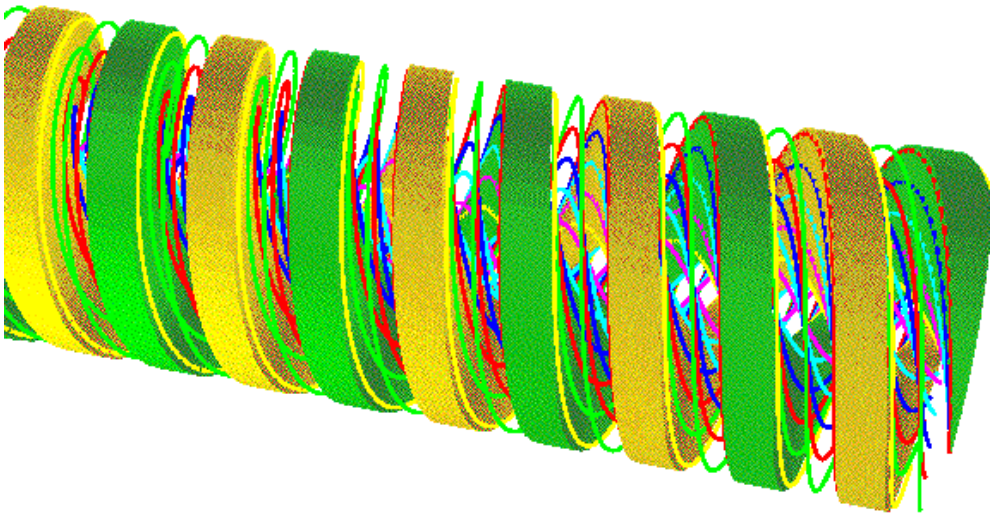

Figure 2 Solid model of the undulator as it is used in the numerical calculations with current filaments and iron between the conductors.

A cross-section of the upper half of a helical undulator with the double helix of iron between the coils and a return yoke is shown in Figure 3. As it was necessary to model at least 6 periods of the undulator to be able to discount the end effects, a great deal of both computer time and space were needed. Thus a two dimensional model was used for the preliminary optimization of the coil height, coil width and yoke height. As r-z coordinates would imply that opposite poles have the same polarity, x-y coordinates were used

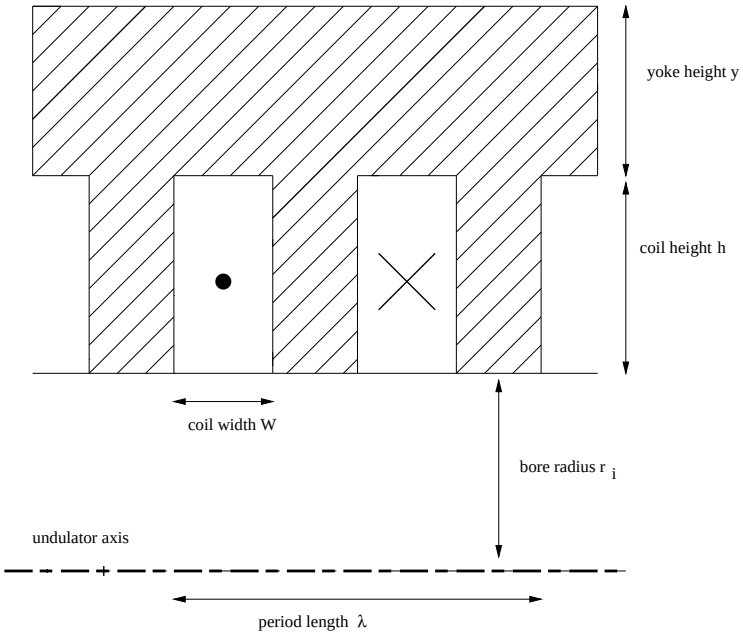

Figure 3 Cross-section of an undulator with iron between the conductors and return yoke (shaded area).

meaning an infinitely wide wiggler. Although this is rather far from the actual helical geometry, the results were reasonable enough to provide the starting parameters for the 3D optimization.
A model was then chosen, using the most promising 2D configuration as a starting point.
For the three dimensional calculations the current in the superconducting coils has to be distributed among a number of filaments. The filaments which are used in the program to simulate the coil do not have to be particularly close together but very careful discretisation and placing of these filaments was necessary to ascertain the effect of varying the coil height and width. Particular care was needed when varying the coil height. The mesh had to be exactly adjusted so that the same current always flowed in the filaments, as, when this was not the case, the variation of current close to the axis had an additional effect on the on-axis field, even though the integrated current density was the same. For each increment in coil height which was calculated, three extra mesh cells and a new row of filaments were added.

Optimization of the geometrical dimensions

The radial on-axis field B_r as function of the coil height *h* is shown in Figure 4. Table 1 lists associated parameters. The field depends strongly on the coil height up to about 4mm after which the curve begins to level off.

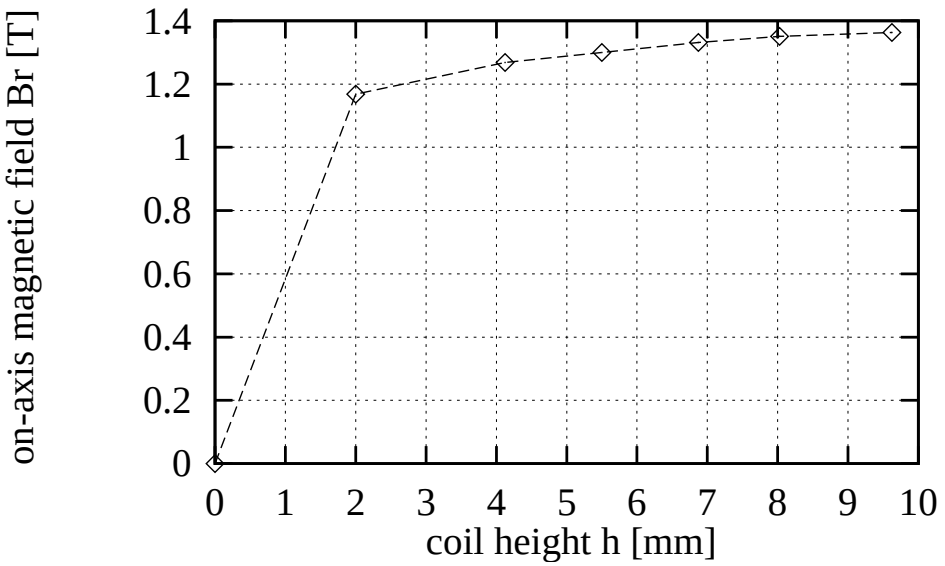

Figure 4 Radial magnetic field amplitude B_r as function of the coil height *h*.

coil height h mm	B_r T	current per filament A	number of filaments
2.0	1.168	337.20	15
4.126	1.268	1160.570	9
5.500	1.300	1160.156	12
6.873	1.331	1159.830	15
8.025	1.350	1159.876	18
9.624	1.363	1159.976	21

Table 1 3D-Optimization for coil height: coil width w=2.81mm, yoke height y=5mm.

Table 2 shows the values obtained from the optimization of the coil width w (which also fixes the thickness of the iron helix). The optimum values are similar to those of the two dimensional simulation.

coil width w mm	B_r T	current per filament A	number of filaments
2.1863	1.2404	901.58	15
2.8125	1.3313	1159.83	15
3.4356	1.2288	1416.79	15

Table 2 3D-Optimization for coil width: coil height h=6.87mm, yoke height y=5mm.

Varying the yoke height y from 3mm to 7mm had very little effect on the on-axis B_r field, even though there was considerable saturation. The maximum permeability in the yoke, varied between 30 and 50.

Table 3 summarizes the optimized undulator parameters. For comparison the parameters of an undulator with equal period but without iron are given.

	undulator with iron	undulator without iron
undulator period λ	10.0 mm	10.0 mm
inner radius r_i	2.0 mm	2.0 mm
coil width w	2.8 mm	3.3 mm
coil height h	5.5 mm	4.0* mm
yoke height y	5.0 mm	–
on-axis field B_r	1.3 T	0.62 T

* At this coil height the on axis magnetic field reaches 90 % of the field of a coil of infinite height.

Table 3 Optimized parameters for an undulator with iron in comparison with an iron free undulator. The current density is 900 A/mm^2.

The magnetic field is increased by more than a factor of 2 due to the iron and the optimized geometry. The coil of the undulator with iron is somewhat narrower as the coil of the undulator without iron. Before further improvements will be discussed in the next chapter, the implications of the new undulator parameters on the positron source will be shown.

To first order the production of an undulator based positron source can be considered as a convolution of the energy dependent cross section for pair production and the spectrum of the undulator.

The threshold for pair production is twice the rest mass of an electron, i.e. 1MeV. The cross section increases with increasing energy up to about 20MeV. Above 20MeV it stays constant and is proportional to the radiation length of the material. Thus for the positron source one is interested in photon energies of 15-25MeV. Photons with energies above ~30MeV contribute to the production of positrons, however, the positrons are produced with a broad energy distribution extending up to the photon energy. The high energy part of the positron spectrum cannot be effectively captured in the capture optics behind the production target and hence does not contribute to the overall yield of the positron source.

The radiation of a helical undulator is considered as the superposition of harmonic radiation bands and is characterized by two quantities: The energy of the first harmonic E_1 and the K-value. The K-value defined as

$$K = 0.934 \cdot B[T] \cdot \lambda[cm]$$

is a measure of the harmonic content of the radiation. The higher the K-value the higher the harmonic content of the radiation, i.e. the broader the spectrum. The energy of the first harmonic is given by:

$$E_1 = \frac{2hc \cdot \gamma^2}{\left(1 + K^2\right)\lambda}$$

h = Planck constant

c = speed of light

γ = Lorentz factor of electron beam

The radiation spectrum peaks at the energy of the first harmonic. Extensive numerical simulations of the positron production and the capture process have revealed an optimum yield with undulator parameters of E_1=20-25MeV and K=1-1.5 [2].

The optimized geometry presented above gives : K=1.26, E_1=23MeV at an electron beam energy of 250GeV. In order to operate the positron source down to an energy of 120GeV electron beam energy an undulator length of ~100 m would be required.

Discussion of possible improvements

The maximum current density that can be reached in a superconducting cable depends on numerous parameters of the cable to be used, such as the copper to superconductor ratio, the number of strands and the size of the gaps between them, the thickness of the insulating material, the manufacturing process of the cable, the magnetic field at the cable and the temperature. Therefore the maximum current density cannot be determined without a detailed technical design of the magnet. It should be noted that a cable for a

helical undulator might look quite different to a cable for dipole or quadrupole magnets. The small bending radius favours the use of thin bands as cable rather than a conventional cable made of strands. Due to the strong dependence of the field on the radius one might try to obtain the highest current density close to the undulator axis, while a lower current density, i. e. a higher amount of copper in the cable could be tolerated further outside. We have restricted our calculations to a current density of 900A/mm^2, a number based on our experience with the HERA magnets. The maximum field at the conductor, that limits the allowable current density, is found to be only 2.9T. Recent developments in the field of fabrication techniques (APC-technique [5]) indicate considerable improvements in the tolerable current density especially at low fields. With a higher current density the undulator period and the overall undulator length could be further reduced. Table 4 lists undulator parameters for a period length of 8mm. The coil width and coil height have been scaled from the 10mm device with the wave length, as it is suggested by equation 1 for the case of an iron free undulator. A current density of 1700A/mm^2 is necessary to reach the desired field of 1.5T. This undulator would allow the operation of the positron source to start with an electron energy of 100GeV. A different approach would be to increase the bore radius of the undulator in order to facilitate the construction and the operation of the device. Increasing the bore radius from 2mm to 2.5mm, while leaving all other parameters as presented in Table 3, would require a current density of 1500A/mm^2 for a field of 1.3T. In this case the field at the conductor is found at 3.2T.

undulator period λ	8.0 mm
inner radius r_i	2.0 mm
coil width w	2.24 mm
coil height h	4.4 mm
yoke height y	5.0 mm
current density I	1700A/mm^2
on-axis field B_r	1.5 T

Table 4 Parameters for an undulator with reduced period length.

Field profile and tracking results

The radial on-axis magnetic field of an undulator with the specified dimensions is a purely harmonic function of the longitudinal coordinate. No contributions of higher harmonics could be resolved within the resolution of the simulations. Figure 5 shows the radial field amplitude as function of the radial position in comparison with an analytic result for an iron free undulator [3]. The field increases with increasing radius, but not as strongly as in the case of the iron free undulator. The dotted line shows a simplified analytical approximation that fits the field of the iron loaded structure even better than the exact result of the iron free undulator.

The approximated field is given by [3]:

$$B_x = -B_0\left[\left(1+\tfrac{1}{8}k^2(3x^2+y^2)\right)\sin(kz) - \tfrac{1}{4}k^2 xy\cos(kz)\right]$$

$$B_y = B_0\left[\left(1+\tfrac{1}{8}k^2(x^2+3y^2)\right)\cos(kz) - \tfrac{1}{4}k^2 xy\sin(kz)\right]$$

$$B_z = -B_0\left(1+\tfrac{1}{8}k^2(x^2+y^2)\right)\left(x\cos(kz)+y\sin(kz)\right)$$

$$k = \tfrac{2\pi}{\lambda}$$

B_0 = on-axis field amplitude

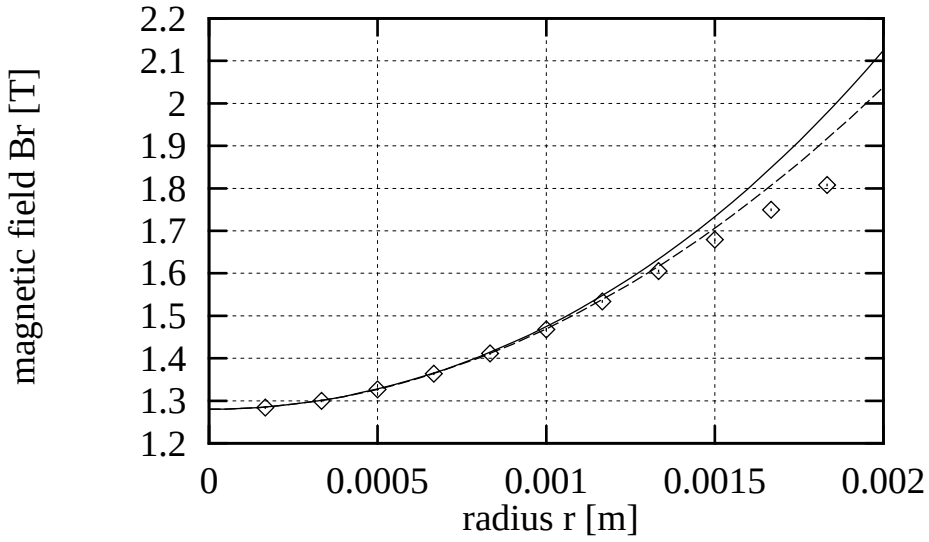

Figure 5 Radial magnetic field as function of the radius (diamonds) in comparison to the field of an iron free undulator (solid line) and a simplified approximation (dashed line).

Particles close to the axis move on helical trajectories with a radius r given by:

$$r = \frac{1}{k^2\rho}$$

where ρ is the cyclotron radius of the particle in the field B_0:

$$\rho = \frac{m_0\gamma c}{eB_0}$$

For a 250GeV electron the radius r is 4nm at a field of 1.3T. Off axis particles move through a somewhat higher field with an additional field gradient. The trajectory becomes an elliptical helix. Both half-axes are a little bit larger than the on-axis radius due to the higher field. The eccentricity amounts to ~12% for an offset of 1mm.

The radiation of an helical undulator is circularly polarized only near the radiation axis, while radiation emitted at angles larger than ~K/γ is transversely polarized. In order to be able to scrape off the transversely polarized radiation it is necessary that the electron

beam is focused through the undulator onto the conversion target, so that the spot size of the radiation on the target is dominated by the opening angle of the radiation. This requires, besides an excellent beam emittance of the order ~10^{-10} πm, that no focusing occurs within the undulator so that the particles move, averaged over a period, on a straight line. The tracking calculations show that the natural focusing of the undulator is so weak that it can be completely neglected for the positron source.
The trajectories in the helical undulator are, however, strongly influenced by the edge field at the entrance of the undulator. Nonlinear kicks can occur if the field is not properly designed.
In the tracking simulations the end field was modeled by a tapered onset of the field given by:

$$B_0 = \frac{1.35T}{1+\exp\left(\frac{-z}{0.002m}\right)}$$

Figure 6 shows the onset of the transverse field component B_y. With this end field only a dipole kick of ~0.4μrad occurs at the entrance of the undulator which can easily be compensated. No detailed calculations of the real end field of the undulator have been performed since the end field is closely connected to the technical design of the undulator. The calculations show, however, that the nonlinearity of the kick at the entrance of the undulator can be sufficiently reduced, if the end field is appropriately tapered.

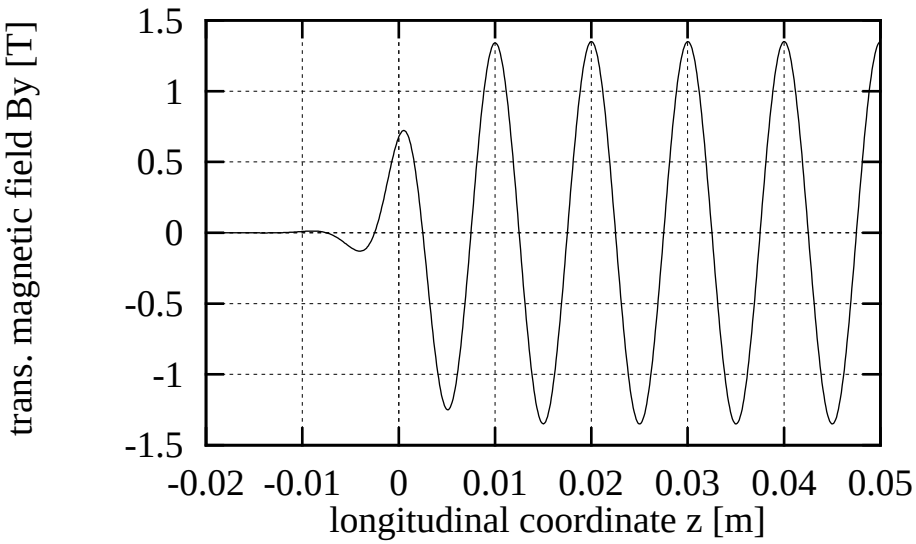

Figure 6 The tapered end field of the helical undulator as it is used in the tracking calculations.

Acknowledgment

We would like to thank W. Decking who provided the code for the tracking calculations.

References

1 V. E. Balakin, A. A. Mikhailichenko 'The Conversion System for obtaining high polarized electrons and positrons', Preprint INP 79-85, 1979.
2 K. Flöttmann, 'Investigations Toward the Development of Polarized and Unpolarized High Intensity Positron Sources for Linear Colliders' DESY 93-161, Nov. 1993.
3 J. P. Blewett, R. Chasman 'Orbits and fields in the helical wiggler' Journal of Applied Physics, Vol.48, No.7, July 1977.
4 The MAFIA Collaboration 'Users's Guide MAFIA Version 3.2' CST GmbH, Lauteschlägerstr. 38, 64289 Darmstadt, Germany.
5 R. M. Scanlan et al 'Evaluation of APC NbTi Superconductor in a Model Dipole Magnet' IEEE Trans. on Magnetics, Vol.30, No.4, July 1994.